Temperature-dependent exciton polariton photoluminescence in ZnO films

A. A. Toropov, O. V. Nekrutkina, and T. V. Shubina
A. F. Ioffe Physico-Technical Institute, Russian Academy of Sciences, St. Petersburg 194021, Russia

Th. Gruber and C. Kirchner
Abteilung Halbleiterphysik, Universität Ulm, 89081 Ulm, Germany

A. Waag
Institute of Semiconductor Technology, Braunschweig Technical University, 38106 Braunschweig, Germany

K. F. Karlsson, P. O. Holtz, and B. Monemar
Linköping University, S-581 83 Linköping, Sweden

(Received 2 December 2003; revised manuscript received 27 January 2004; published 16 April 2004)

The polarized photoluminescence (PL) in a (0001) oriented ZnO epitaxial film is studied in the temperature range 4.5–250 K. We report the evidence of exciton polariton emission between 50 and 130 K. In this range the PL of mixed polariton modes is detected in the geometry of an extraordinary beam, realized by the use of a large-aperture microobjective collecting light from the cleaved sample edge at different angles with respect to the **c** axis. The elevated temperatures facilitate the polariton emission due to the thermal population of both A and B exciton branches and the enhanced polariton scattering into the photonlike mixed modes.

DOI: 10.1103/PhysRevB.69.165205 PACS number(s): 71.36.+c, 78.55.Et

ZnO is a semiconductor compound with remarkably large exciton and biexciton binding energies ($\sim$60 meV and $\sim$15 meV, respectively) as well as exciton longitudinal-transverse splitting ($\sim$1.5 meV for the A exciton and 10–12 meV for the B and C excitons). The excitonic properties of ZnO bulk crystals have been intensively studied since the 1960s.[1–5] Recently the interest in excitons for the column two oxides (ZnO, MgO, CdO) and their solid alloys has been renewed due to the observation of high-temperature stimulated excitonic emission in ZnO based superlattices[6] and the intensive search of excitonic media suitable for fabrication of high-temperature devices based on microcavity polaritons.[7] These works have stimulated the studies of exciton polaritons in ZnO at elevated temperatures. In spite of the well documented excitonic character of the ZnO photoluminescence (PL) up to room temperature,[8,9] most of the published data on exciton polaritons are limited to cryogenic temperatures. This is probably because the temperature-dependent PL has typically been measured in the so-called α geometry ($\mathbf{k}\|\mathbf{c}$, $\mathbf{E}\perp\mathbf{c}$), where **k** is the light wave vector, **E** is the electric field vector, and **c** is the principal axis of the wurtzite crystal. This geometry is inconvenient for the studies of polaritonic effects since the observation of both A and B longitudinal Γ_5 excitons in ZnO are not allowed in this case (see, e.g., Ref. 10).

The effects of longitudinal excitons are frequently considered as the manifestation of the polaritonic nature of excitonic spectra.[10,11] In a hexagonal crystal, such as ZnO, the longitudinal excitons can be detected in the geometry of an extraordinary beam (mixed polariton mode). In this geometry light is polarized in the plane containing both the **c** axis and **k**, as illustrated in Fig. 1. Usually, angle ϕ between **k** and the direction perpendicular to **c** is small so that the experimental geometry is close to the so-called π polarization scheme ($\mathbf{k}\perp\mathbf{c}$, $\mathbf{E}\|\mathbf{c}$), when all other excitonic transitions in the region of the lowest-energy A and B excitons in ZnO are either forbidden or weak.

In this paper we study the linearly polarized edge emission in an epitaxial thin film of ZnO, clearly demonstrating polaritonic effects up to the temperatures of $\sim$130 K. The studied sample was a 1.2 μm thick layer of ZnO grown by metal organic chemical vapor deposition on the (0001) plane of a GaN template deposited above a sapphire substrate.

PL studies were carried out both from the sample surface and from the cleaved sample edge. A microphotoluminescence (μ-PL) setup was used in the latter case. The surface PL and PL excitation (PLE) spectra were detected using a 325 nm line of a He-Cd laser or an emission of a Xe lamp passed through a monochromator. The μ-PL technique was described in detail elsewhere.[12] For most of the μ-PL measurements the excitation power was 17 μW just before the cryostat window. The beam (a cw 266 nm laser line) propagating normal to the sample cleaved edge was focused by a reflective objective into a spot of $\sim$1 μm in diameter. The spot size allowed us to excite selectively ZnO, without touching GaN, this was checked by monitoring the GaN near-band-gap emission spectrum. The PL signal was dispersed by a monochromator and detected by a nitrogen-

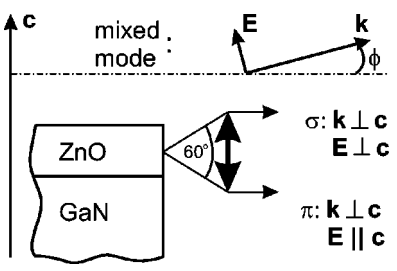

FIG. 1. Schematic view of the μ-PL measurement geometry.

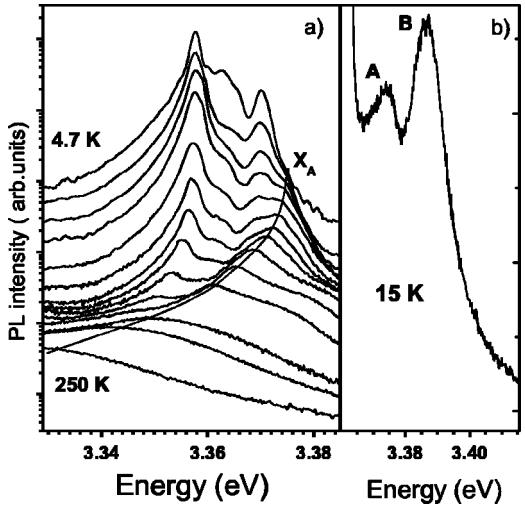

FIG. 2. (a) Surface PL spectra (α polarization) for a set of temperatures between 4.7 and 250 K. The PL intensity is shown in a logarithmic scale. For demonstrative purpose the spectra are vertically offset. (b) The PLE spectrum at 15 K.

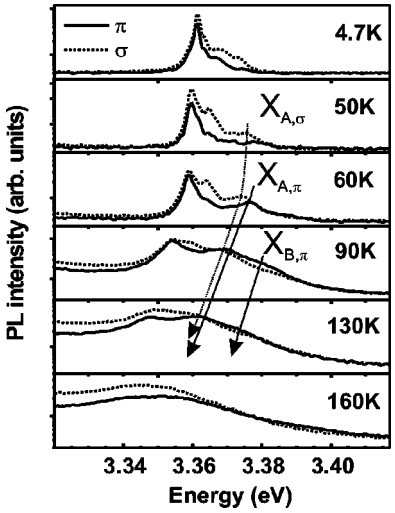

FIG. 3. Edge PL spectra (σ and π polarizations) measured at different temperatures. The PL intensity is shown in a logarithmic scale.

cooled charge-coupled device camera. A linear polarizer (followed by a depolarizer) was mounted between the objective and the monochromator. One should note that the numerical aperture of the objective (NA=0.5) resulted in the collection of light within $\pm 30°$ from the normal to the surface, as shown schematically in Fig. 1.

Figure 2(a) demonstrates the surface PL spectra (α geometry) measured at different temperatures. A number of bound exciton lines are visible in the low-temperature spectra, as well as a weak free-exciton emission line (X_A). The temperature rise leads to an increase in the X_A relative intensity so that it becomes a dominant line at the temperatures higher than 120–150 K, in good agreement with the previously reported data.[8] In the following discussion we will focus mainly on the spectral region of the free-exciton emission. Figure 2(b) shows the PLE spectrum detected at the maximum of the most intensive bound exciton peak. Both A and B free-exciton peaks are well resolved in the spectrum, allowing estimation of the exciton resonance energies. Figure 3 displays the PL spectra measured at different temperatures from the cleaved sample edge ($\mathbf{k}\perp\mathbf{c}$) for σ ($\mathbf{E}\perp\mathbf{c}$, dotted curves) and π ($\mathbf{E}\|\mathbf{c}$, solid curves) polarizations (see the drawing in Fig. 1). At low temperatures all the peaks of bound excitons are σ polarized with different degrees of polarization. Starting from 20–40 K the well-resolved free-exciton peak appears ($X_{A,\sigma}$), being visible uniquely in σ polarization. The further temperature increase above 50–60 K results in the appearance of another peak $X_{A,\pi}$, which is dominantly π polarized, at the energy 2–3 meV above the lowest-energy free-exciton peak. At even higher temperatures, a PL tail emerges from the higher-energy side for σ polarization, and one more relatively wide smooth peak $X_{B,\pi}$ appears for π polarization. Above 130–150 K the emission peaks are severely broadened due to the interactions with phonons, so that no fine excitonic structure can be resolved.

The low-temperature free-exciton PL spectra in ZnO crystals were previously studied at $\mathbf{k}\perp\mathbf{c}$ for both σ and π polarizations.[13] Our low-temperature spectra (<50 K) are in general agreement with the published data. The lowest-energy strong exciton is a transverse A exciton with Γ_5 symmetry, which contributes uniquely to the PL with $\mathbf{E}\perp\mathbf{c}$ (α or σ geometries). In the $\mathbf{E}\|\mathbf{c}$ geometry (π polarization) both A and B excitons should be much weaker, since they are a weakly allowed Γ_1 exciton and a forbidden Γ_6 exciton. The Γ_1 exciton is an A exciton and the Γ_6 exciton is a B one if we accept the Γ_7(A) - Γ_9(B) - Γ_7(C) valence bands ordering in ZnO, as adopted by most of the researchers (see the discussion in Ref. 14, and references therein). The alternative ordering of the valence bands Γ_9(A) - Γ_7(B) - Γ_7(C), which was also proposed,[15–17] results in an A Γ_6 exciton and B Γ_1 exciton. In any case the dominance of $\mathbf{E}\perp\mathbf{c}$ light polarization is expected, with only small (if any) admixture of light with $\mathbf{E}\|\mathbf{c}$. This is exactly what we observe at low temperatures. However, the observation at elevated temperatures of quite strong π polarized lines is unexpected because the lowest-energy strong exciton available in this geometry is a C Γ_1 exciton which appears at much higher energy ($\sim$3.425 eV). To explain the emergence of these peaks we resort to the exciton-polariton concept.

Figure 4(a) shows the polariton dispersion curves of ZnO for A and B excitons. To construct this plot we extracted the resonance energies of the transverse Γ_5 excitons ($A\Gamma_5^T$, $B\Gamma_5^T$) from low-temperature PLE spectra measured in the same sample. The values of longitudinal-transverse splittings for A and B excitons were taken from Ref. 13. In Fig. 4(a) we neglect the oscillator strength of the weakly allowed Γ_1 exciton and the forbidden Γ_6 exciton. The validity of this simplification for interpretation of the experimental spectra will be discussed further. In this approximation no oscillator strength is expected for the spectral range of A and B excitons for the pure π polarization ($\mathbf{E}\|\mathbf{c}$). The dash-dotted curves in Fig. 4(a) display the dispersions of excitons and photons, whereas the dotted, dashed, and solid curves represent polaritonic branches, where the exciton-photon coupling

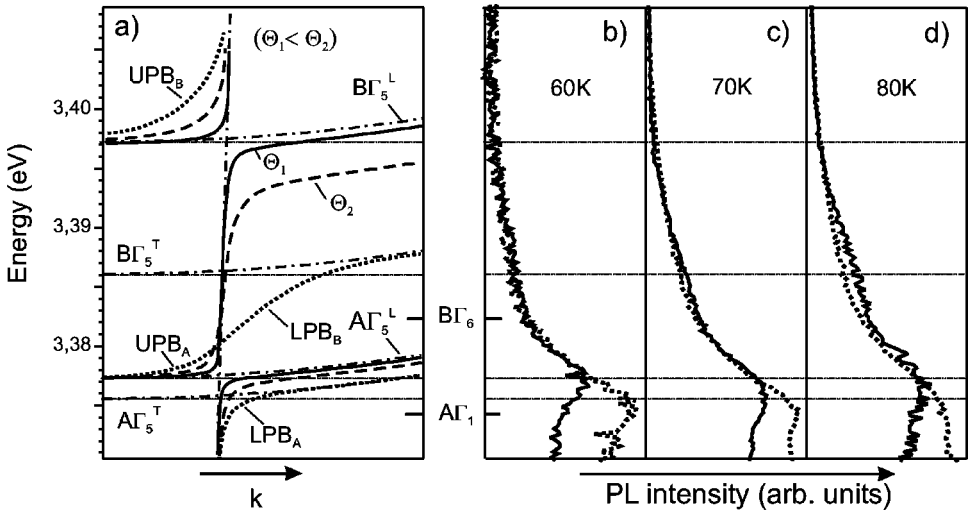

FIG. 4. (a) ZnO polaritonic dispersion curves in the region of A and B excitons. Dotted curves correspond to the polarization of an ordinary beam ($\mathbf{E}\perp\mathbf{c}$). Solid and dashed curves represent the mixed polariton modes allowed in the geometry of an extraordinary beam for two angles Θ (Θ_1—solid curves, Θ_2—dashed curves, $\Theta_1<\Theta_2$). (b)–(d) The PL spectra measured at σ (dotted curve) and π (solid curves) polarizations at the selected temperatures. The energy scales of the spectra are shifted to match the low-temperature energy scale of (a).

is taken into account. Dotted curves correspond to $\mathbf{E}\perp\mathbf{c}$ (α and σ geometries). The only difference between the α and σ geometries concerns the longitudinal excitons ($A\Gamma_5^L$, $B\Gamma_5^L$). They are forbidden in the α geometry due to the absence of dipoles oriented along the **c** axis for Γ_5 excitons. In the σ geometry the longitudinal excitons are allowed. However, they do not interact with photons due to the transverse nature of electromagnetic waves.

Figures 4(b–d) show the linearly polarized μ-PL spectra, measured at three selected temperatures, in the same energy scale as the low-temperature polaritonic dispersion curves [Fig. 4(a)]. For demonstrative purposes the experimental spectra are shifted to compensate the respective temperature induced shifts of the band edge. At 60 K the σ polarized PL peak [the dotted curve in Fig. 4(b)] lies just below the A transverse Γ_5 exciton energy. This is in agreement with the conventional point of view that the polariton luminescence process involves mainly photonlike polaritons from the region of the polariton bottleneck.[18]

Solid and dashed curves in Fig. 4(a) represent the dispersion of mixed polariton modes observed in the geometry of an extraordinary beam (see Fig. 1).[10,11] Let Θ be the angle between a vector normal to the **c** axis and the wave vector **k** of the photon inside the crystal. $\Theta=0$ corresponds to the π geometry with an unobservable purely longitudinal exciton. At a finite angle Θ the longitudinal exciton couples to the electromagnetic field due to the non-zero projection of the extraordinary field on the direction of vector **k** inside the crystal. The strength of the exciton-photon coupling for the mixed mode is proportional to $(\sin^2\Theta)$.[10] As Θ increases from 0, the lower mixed polariton branches shift to lower energy from the energy of the respective longitudinal exciton, while the upper branches display a greater curvature as a result of the enhanced coupling. Finally, we arrive at $\Theta=90°$ to the α geometry with a purely transverse exciton. The two sets of mixed polariton branches are shown in Fig. 4(a) for two different angles Θ ($\Theta_1<\Theta_2$). Note that the light polarization $\mathbf{E}\perp\mathbf{c}$ implies propagation of an ordinary beam with the purely transverse polarization of the electric-field vector inside the crystal for any Θ.

The occurrence of the mixed modes could explain the appearance of the PL signal when detecting the $\mathbf{E}\|\mathbf{c}$ polarized light. An important factor facilitating this observation is the use of a microobjective with large numerical aperture. The emission is in fact collected within a certain angle around the surface normal, thus allowing detection of the mixed polariton modes spreading in the crystal with $\Theta<\Theta_{cr}$. For our experimental conditions Θ_{cr} can be estimated as $5-10°$. The estimation accuracy is poor due to the uncertainty in the ZnO refractive index value within the polaritonic region. Nevertheless, there is no doubt that the large-aperture optics can allow the observation of the mixed polariton modes in the geometry which at first sight might have been expected to provide only the detection of purely π polarized light.

The lowest-energy "π polarized" peak [see solid curves in Figs. 4(b–d)] appears at 50–60 K slightly below the energy of the A longitudinal exciton. The temperature increase results in a peak broadening and the appearance of another smooth π polarized peak in the gap between the A and B Γ_5 longitudinal excitons. With the temperature increase this second peak gains intensity and simultaneously shifts to higher energies. By their energy positions, the peaks can be assigned to the emission from the thermally populated mixed polariton modes. Indeed, comparing Figs. 4(a) and 4(b–d), one can notice a clear correspondence between the expected region of the polariton bottleneck for the A exciton mixed polariton modes with reasonably small Θ and the position of the lowest π polarized peak. The situation with the B exciton is more complicated. The transverse B exciton lower polariton branch (LPB_B) is combined with the A exciton upper polariton branch (UPB_A) [see Fig. 4(a)]. Therefore, the bottleneck region is smoothed out due to the absence of a purely photonlike region. The effect should be especially important for ZnO, where the B exciton longitudinal-transverse splitting is comparable with the gap between the A and B transverse excitons. This is apparently the reason why there is no strong spectral feature relevant to the B exciton in the σ polarized emission at any temperature. The curvature of the mixed polariton branches at relatively small Θ is smaller and the bottleneck is shaped better. Then the shape of the respective π polarized emission spectrum in this region should be

determined simultaneously by the thermal distribution of excitons and the angle distribution of the mixed mode emission collected by the optics. Note that the direct thermal population is efficient only for excitonlike regions of the dispersion curves due to the small density of states for photonlike excitons.

The detection of mixed polariton modes due to the large-aperture optics explains qualitatively the observation of π polarized emission peaks within the gap between the transverse and longitudinal excitons both for A and B excitons. Nevertheless, let us think about other possible mechanisms which could result in the emergence of such peaks. First of all, one should consider contributions from the weakly allowed Γ_1 exciton and the forbidden Γ_6 exciton. Both of them were observed in wurtzite crystals in the π polarization, when the strong Γ_5 excitons are completely forbidden.[11,16,19] This attribution in ZnO can be somewhat confusing if to have in mind the existent controversy concerning the valence bands ordering. As for the A exciton, the assignment of the lower-energy π polarized peak observed in this work to the emission of such an exciton is not possible, because the energy position of the latter should be below the A Γ_5 transverse exciton energy for either ordering scheme. The B exciton (either Γ_6 or Γ_1) energy falls within the lower-energy tail of the upper lying wide π polarized peak [see Fig. 4 for the case of the Γ_7(A)-Γ_9(B)- Γ_7(C) ordering scheme] and certain contribution from this exciton appears to be possible. However, the respective lines observed previously for the weakly allowed or forbidden excitons were relatively narrow, which does not correlate with the large spectral width of the observed peak, covering most of the gap between the transverse and longitudinal B excitons ($\sim$11 meV). Therefore, the appearance of Γ_6 or Γ_1 excitons could hardly explain the emergence of the two discussed spectral features.

An additional factor resulting in the enhanced emission of the mixed modes visible in the π polarization can be the nonelastic scattering of the extraordinary polaritons due to the collisions with acoustical phonons and impurities. The scattering events can change direction of the polaritons, i.e., change Θ. Especially advantageous should be the interband scattering between the mixed modes towards smaller Θ, because this process transfers the excitonlike polaritons from the thermal distribution into the photonlike polaritons, which can easily escape the crystal. Similar interband scattering mechanism was previously applied to explain a π polarized feature in the edge emission spectrum of high-quality films of GaN.[12] The exact contribution of this process is not clear at present.

In conclusion, we have observed emission of mixed polariton modes in ZnO in the temperature range of 50–130 K. The elevated temperature seems to be important both to establish the thermal distribution of excitons and to enhance the phonon induced polariton scattering into the photonlike modes.

This work was partly supported by the Program of the Ministry of Sciences of RF ''Physics of Solid State Nanostructures'' and RFBR Grant No. 04-02-17652.

[1] D.G. Thomas, J. Phys. Chem. Solids **15**, 86 (1960).
[2] J.J. Hopfield, J. Phys. Chem. Solids **15**, 97 (1960).
[3] J.J. Hopfield and D.G. Thomas, Phys. Rev. Lett. **15**, 22 (1965).
[4] G. Blattner, G. Kurtze, G. Schmieder, and C. Klingshirn, Phys. Rev. B **25**, 7413 (1982).
[5] J.M. Hvam, G. Blattner, M. Reuscher, and C. Klingshirn, Phys. Status Solidi B **118**, 179 (1983).
[6] A. Ohtomo, K. Tamura, M. Kawasaki, T. Makino, Y. Segawa, Z.K. Tang, G.K.L. Wong, Y. Matsumoto, and H. Koinuma, Appl. Phys. Lett. **77**, 2204 (2000).
[7] M. Zamfirescu, A. Kavokin, B. Gil, G. Malpuech, and M. Kaliteevski, Phys. Rev. B **65**, 161205 (2002).
[8] D.W. Hamby, D.A. Lucca, M.J. Klopfstein, and G. Cantwell, J. Appl. Phys. **93**, 3214 (2003).
[9] L. Wang and N.C. Giles, J. Appl. Phys. **94**, 973 (2003).
[10] J.J. Hopfield and D.G. Thomas, J. Phys. Chem. Solids **12**, 276 (1960).
[11] C. Benoit a la Guillaume, A. Bonnot, and J.M. Debever, Phys. Rev. Lett. **24**, 1235 (1970).
[12] T.V. Shubina, T. Paskova, A.A. Toropov, S.V. Ivanov, and B. Monemar, Phys. Rev. B **65**, 75 212 (2002).
[13] S.F. Chichibu, T. Sota, G. Cantwell, D.B. Eason, and C.W. Litton, J. Appl. Phys. **93**, 756 (2003).
[14] A.V. Rodina, M. Strassburg, M. Dworzak, U. Haboek, A. Hoffman, A. Zeuner, H.R. Alves, D.M. Hofmann, and B.K. Meyer, Phys. Rev. B **69**, 125206 (2004).
[15] Y.S. Park, C.W. Litton, T.C. Collins, and D.C. Reynolds, Phys. Rev. **143**, 512 (1966).
[16] D.C. Reynolds, D.C. Look, B. Jogai, C.W. Litton, G. Cantwell, and W.C. Harsch, Phys. Rev. B **60**, 2340 (1999).
[17] B. Gil, Phys. Rev. B **64**, 201310 (2001).
[18] Y. Toyozawa, Prog. Theor. Phys. Suppl. **12**, 111 (1959).
[19] J.J. Hopfield and D.G. Thomas, Phys. Rev. **122**, 35 (1961).